Cancer Chemotherapy and Pharmacology (2023) 92:341–355
https://doi.org/10.1007/s00280-023-04571-2

ORIGINAL ARTICLE

Quantitative proteomics profiling reveals the inhibition of trastuzumab antitumor efficacy by phosphorylated RPS6 in gastric carcinoma

Chun-Ting Hu[1] · Shao-Jun Pei[3,4] · Jing-Long Wang[1] · Li-Dong Zu[1] · Wei-Wei Shen[1] · Lin Yuan[5] · Feng Gao[5] · Li-Ren Jiang[5] · Stephen S.-T. Yau[2,4] · Guo-Hui Fu[1]

Received: 24 March 2023 / Accepted: 17 July 2023 / Published online: 28 July 2023

Abstract

Background The anti-HER2 antibody trastuzumab is a standard treatment for gastric carcinoma with HER2 overexpression, but not all patients benefit from treatment with HER2-targeted therapies due to intrinsic and acquired resistance. Thus, more precise predictors for selecting patients to receive trastuzumab therapy are urgently needed.

Methods We applied mass spectrometry-based proteomic analysis to 38 HER2-positive gastric tumor biopsies from 19 patients pretreated with trastuzumab (responders $n=10$; nonresponders, $n=9$) to identify factors that may influence innate sensitivity or resistance to trastuzumab therapy and validated the results in tumor cells and patient samples.

Results Statistical analyses revealed significantly lower phosphorylated ribosomal S6 (p-RPS6) levels in responders than nonresponders, and this downregulation was associated with a durable response and better overall survival after anti-HER2 therapy. High p-RPS6 levels could trigger AKT/mTOR/RPS6 signaling and inhibit trastuzumab antitumor efficacy in nonresponders. We demonstrated that RPS6 phosphorylation inhibitors in combination with trastuzumab effectively suppressed HER2-positive GC cell survival through the inhibition of the AKT/mTOR/RPS6 axis.

Conclusions Our findings provide for the first time a detailed proteomics profile of current protein alterations in patients before anti-HER2 therapy and present a novel and optimal predictor for the response to trastuzumab treatment. HER2-positive GC patients with low expression of p-RPS6 are more likely to benefit from trastuzumab therapy than those with high expression. However, those with high expression of p-RPS6 may benefit from trastuzumab in combination with RPS6 phosphorylation inhibitors.

Keywords Trastuzumab · Ribosomal protein S6 · Gastric carcinoma

Introduction

The National Cancer Center of China reports that gastric cancer (GC) is the third most common cancer and the third-leading cause of cancer-related deaths for both sexes [1]. HER2 (also known as ERBB2) overexpression

Chun-Ting Hu and Shao-Jun Pei have contributed equally to this work.

✉ Stephen S.-T. Yau
yau@uic.edu

✉ Guo-Hui Fu
guohuifu@shsmu.edu.cn

[1] Department of Pathology, Faculty of Basic Medicine, Key Laboratory of Cell Differentiation and Apoptosis of Chinese Ministry of Education, Institutes of Medical Sciences, Shanghai Jiao Tong University School of Medicine, Shanghai, China

[2] Yanqi Lake Beijing Institute of Mathematical Sciences and Applications (BIMSA), Huairou District, Beijing 101400, People's Republic of China

[3] School of Public Health, Peking University, Beijing 100191, People's Republic of China

[4] Department of Mathematical Sciences, Tsinghua University, Beijing 100084, People's Republic of China

[5] Pathology Center, Shanghai General Hospital, Shanghai Jiao Tong University School of Medicine, Shanghai, China

occurs in approximately 21.2–22.1% of gastric cancer [2, 3], but this rate is even lower of 13% in four representative Chinese clinical centers [4]. Although the anti-HER2 antibody trastuzumab is effective in gastric cancer patients with HER2 overexpression, the median overall survival (OS) time is 10–35 months, and the response greatly varies [5–7]. Additionally, HER2 status is not an independent prognostic factor for Chinese gastric cancer patients [4]. Intratumor, intrapatient, and interpatient heterogeneity in gastric cancer are the main barriers to the effectiveness of trastuzumab targeted therapy [8]. Therefore, more research on effective predictors for a durable response to trastuzumab therapy in HER2-overexpressing gastric carcinoma is needed.

Although many large-scale DNA sequencing studies have focused on the molecular characterization of gastric cancer to identify dysregulated oncogenic pathways and cancer driver gene mutations at the genomic level [9], knowledge regarding their impact on gastric cancer targeted therapy is limited [10]. The central importance of disease pathogenesis and all existing drug targets are proteins that represent intermediate phenotypes for disease and are linked to clinical outcomes [11, 12]. There are a number of studies using the quantitative proteomics approach to assess trastuzumab resistance [13, 14], the effects of trastuzumab on kinase activity in gastric cancer cell lines [15], and HER2 status to identify patients who would benefit from trastuzumab [16]. In contrast to the extensive effects of trastuzumab in GC cell line research, deep proteomic analysis of tumor histological samples of GC patients has not yet been performed.

Here, we prospectively collected pretreated tumor samples of GC patients who were treated with trastuzumab and divided them into two cohorts (responders and nonresponders) based on the patients' clinical parameters of response to trastuzumab. We compared the proteomics of the two cohorts using three approaches: (1) analysis of differentially expressed proteins (DEPs) across the two cohorts coupled with Gene Ontology (GO) term enrichment and Kyoto Encyclopedia of Genes and Genomes (KEGG) pathway analysis, (2) gene set enrichment analysis (GSEA) and gene set variation analysis (GSVA) of differentially expressed genes, and (3) principal component analysis (PCA) to explore explicit function differences between the responders and the nonresponders. We found that phosphorylated RPS6 (p-RPS6) is differentially expressed in responders and nonresponders, and low p-RPS6 expression is significantly associated with better response and survival after anti-HER2 therapy. We identified that p-RPS6 can be offered as a potential pretreatment predictor of a durable response to trastuzumab therapy and better survival in HER2-positive gastric carcinoma patients.

Materials and methods

Proteomics patient samples

HER-2-positive patients who received trastuzumab treatment were enrolled in this study, and 19 tumor specimens and their matched normal tissues were taken shortly before the initiation of the treatment. Patients were categorized into responders and nonresponders, as evaluated by standard Response Evaluation Criteria in Solid Tumors (RECIST v1.1) guidelines.

All formalin-fixed and paraffin-embedded (FFPE) patient tissues were sliced (10 μm thick) and ensured > 70% of tumor cell content for LC−MS/MS analysis. The specimens in this study were obtained with the approval of The Shanghai General Hospital Affiliated of Shanghai Jiaotong University review boards. The overall survival (OS) of all patients was followed up with a median period of 30 months, which was calculated from the date of trastuzumab treatment to the date of mortality or the last follow-up.

LC−MS/MS-based proteomics

An Orbitrap Fusion LUMOS mass spectrometer (Thermo Fisher Scientific) coupled with an Easy-nLC 1200 via an Easy Spray (Thermo Fisher Scientific) was used for MS analysis. Peptides were separated with a 2.1*150 mm Ethylene Bridged Hybrid (BEH) C18 3 μm column (Waters) at 40 °C with 0.2 ml/min flow and a 60 min ACN gradient (5 ~ 30%) in 5 mM ammonium formate (pH 10). The peptide mixtures were loaded onto a self-packed analytical PicoFrit column with an integrated spray tip (New Objective, Woburn, MA, USA) (75 μm × 40 cm length) packed with ReproSil-Pur 120A C18-AQ 1.9 μm (Dr. Maisch GmbH, Ammerbuch, Germany) and separated within a 120 min linear gradient from 95% solvent A (0.1% formic acid/2% acetonitrile/98% water) to 28% solvent B (0.1% formic acid/80% acetonitrile) at a flow rate of 250 nl/min at 50 °C. The mass spectrometer was operated in positive ion mode and employed in the data-dependent mode within the specialized cycle time (3S) to automatically switch between MS and MS/MS. One full MS scan from 350 to 1500 m/z was acquired at high resolution $R = 120{,}000$ (defined at $m/z = 400$); MS/MS scans were performed at a resolution of 30,000 with an isolation window of 4 Da and higher energy collisional dissociation (HCD) fragmentation. Data were analyzed in Spectronaut X (Biognosys, Schlieren, Switzerland).

Mass spectrometry data processing

The MS data of the fractionated pools were used to generate a data-dependent acquisition (DDA) spectral library. All the raw data including depleted and undepleted sample with each fraction were analyzed to generate spectral library using the Pulsar search engine (only available in Spectronaut Pulsar). All searches were performed against the human SwissProt fasta databases (42,431 entries downloaded on July 2019) of canonical and isoform sequences. The digestion enzyme was allowed for specific trypsin enzyme with 2 missed specialized cleavages, and carbamidomethyl of cysteine specified as a fixed modification and oxidation of methionine as variable modifications. Fragment ions for the targeted data analysis were selected from 300 to 1800 m/z, minimal relative intensity was set to > 5%, and fragment ion number > 3. A protein false discovery rate (FDR) was set to 1% and peptide spectrum matches. Protein inference was performed using the ID Picker algorithm integrated within the Spectronaut software. For MS/MS acquisition, data-independent acquisition (DIA) method was set 50 variable isolation windows according to the FWTH (full width at half maximum), and the specific windows lists were constructed based on the respective DDA data of the pooled sample. For DIA analysis, the FDR was estimated with the mProphet approach and set to 1% at peptide precursor level and 1% at protein level. The protein intensity was summed by the intensity of their respective peptides which was calculated by the peak areas of their respective fragment ions of MS2. All results were filtered by a Q value cutoff of 0.01 (corresponds to FDR of 1%).

Proteomics statistical analysis

Proteomics statistical analysis was performed by MATLAB (RRID:SCR_001622), R Project for Statistical Computing (RRID:SCR_001905) or Gene Set Enrichment Analysis (RRID:SCR_003199). For the clinical proteomics data, the protein groups with at least 50% valid values were retained, and normalized ratio posttreatment/pretreatment data were log2-transformed. Eventually, 3949 proteins remained and were used for all subsequent analyses. The dataset was integrated by gene name. The missing data were filled by the K-nearest neighbor (KNN) method with $k = 3$. To identify the proteins with different expression levels between responders and nonresponders, a two-sample Student's t test was performed with a p value threshold of 0.05 for two datasets, followed by Gene Set Enrichment Analysis (GSEA) with NOM p value and FDR q-value 0.25 to recognize the upregulated gene sets in each of the two datasets. Principal component analyses (PCA) of each gene set were conducted in R using the FactoMineR package based on normalized ratios of different genes with log2 transformation in the gene sets. The survival analyses were performed in R using the Survival package based on the Cox proportional hazards regression model. Proteomaps (https://www.proteomaps.net/) were constructed using a web tool based on the normalized ratio without log2 transformation.

Sequencing data analysis

Published RNA-sequencing data of four gastric cancer cell lines treated with trastuzumab for 4 or 24 h were downloaded from the GEO database through GEO series accession number GSE141352 (https://www.ncbi.nlm.nih.gov/geo/query/acc.cgi?acc=GSE141352). All RNA data were analyzed using normalized ratio posttreatment/pretreatment with log2 transformation. The gene annotations were added from the GO and KEGG (RRID:SCR_012773) databases. The two-sample Student's t test was performed with a p value threshold of 0.05 between responders and nonresponders in the RNA dataset.

Immunohistochemistry staining and analysis

FFPE tumor blocks were used to assess phosphorylated RPS6 protein in patient tissue. Samples were incubated with primary antibodies targeting p-RPS6 (Cell Signaling Technology, Cat#5364) and RPS6 (Cell Signaling Technology, Cat#2317), and the presence of brown chromogen in the tumor cell indicates positive immunoreactivity. The variables measured included the intensity of staining and the proportion of positively stained cells. The intensity of staining was graded as negative = 0, weak = 1, moderate = 2, or strong = 3. The proportion of positively stained cells was scored as 0% = 0, 1–25% = 1, 26–50% = 2, 51–75% = 3, or 76–100% = 4. The final staining score was calculated as the intensity grade multiplied by the proportion of positively stained cells. Samples with a final staining score of 8 or higher were considered to have high expression according to a receiver-operating characteristic (ROC) curve.

RNA interference, vector construction, and transfection

The cDNA sequence of RPS6 was inserted into the vector of pLX304-Blast-V5 and RNAi plasmid was constructed with the vector pGIPZ for overexpression and knockdown, while the empty plasmids were used as a control. The core interference sequences as follows: shRPS6-1:5′GCATTCCTGTTACAGACCA-3′; shRPS6-2:5 ′CGCCAGTATGTTGTAAGAA3′; shCtrl:5′ GCAACAACGCCACCATAAACT 3′. For the transfection of plasmids, cells were transfected using the Lipofectamine 3000 kit (Invitrogen, USA) according to the manufacturer's instructions.

Cell proliferation assessment

GC cells were seeded onto 96-well culture plates in growth media and precultured for 24 h. The chemical inhibitor GSK458 (omipalisib, MedChemExpress) and trastuzumab were added to the medium at 100 nmol/L and 100 μg/mL, respectively. Cell proliferation was assessed every 24 h for 5 days by Cell Counting Kit-8 (CCK-8, Dojindo, Japan) according to the manufacturer's instructions. At specific time points, CCK-8 reagent was added to each well for 2 h at 37 °C. Then, the absorbance at 450 nm was determined by an iMark microplate reader (Bio-Rad, USA). All experiments were performed in triplicate and repeated three times.

In vivo nude mouse model

Female BALB/c nude mice (4–5 weeks old) were used to perform subcutaneous xenograft experiments. A total of 3×10^6 NCI-N87 cells were subcutaneously injected into the buttock of each mouse. For efficacy studies, treatment started when tumors reached approximately 30–40 mm^3. Mice were divided into four groups randomly and treated with control, trastuzumab (10 mg/kg, twice weekly), GSK458 (1.5 mg/kg, alternate days), or the combination by i.p. injection given for more than 2 weeks. Tumors were measured every 3 days using calipers, and tumor volume was calculated using the formula: 1/2 (length × $width^2$). After treatment, animals were sacrificed and tumors were collected for histology and biochemistry analysis. All procedures involving mice were approved by the Animal Care and Use Committee of the Shanghai Jiao Tong University School of Medicine.

Western blot analysis

For downstream signaling studies, GC cells were pretreated with the inhibitor GSK458 (100 nmol/L), trastuzumab (100 μg/mL), or a combination of both for 24 h and 96 h, washed with ice-cold PBS, and lysed in a cell lysis solution. Blotting of membranes was performed using the following primary antibodies: AKT (Cell Signaling Technology, Cat#4685), phospho-AKT (Cell Signaling Technology, Cat#4058), RPS6 (Cell Signaling Technology, Cat#2317), phospho-RPS6 (Cell Signaling Technology, Cat#5364), β-tubulin (Cell Signaling Technology, Cat#2146), and vinculin (Cell Signaling Technology, Cat#13,901). All antibodies were purchased from Cell Signaling Technology. Proteins were visualized with chemiluminescence detection reagent.

Statistical analysis

All quantitative results for in vitro and in vivo experiments data were presented as the mean ± SD. Comparison between two groups were analyzed using the two-tailed Student's *t* test. Multiple groups' comparison was determined by one-way ANOVA. All statistical analyses were performed with GraphPad Prism (v5.01, GraphPad Software Inc.). For all studies, a p value < 0.05 was considered statistically significant.

Results

Proteomics analysis of gastric carcinoma patient response to trastuzumab therapy

To identify protein networks associated with the response to trastuzumab therapy, we applied quantitative mass spectrometry to analyze 19 treatment-naive primary tumors (from responders, $n = 10$; nonresponders, $n = 9$), and matched normal tissues for each patient as germline references. We divided patients into responders (including those with partial response, PR and complete response, CR) and nonresponders (including those with progressive disease, PD and stable disease, SD) based on RECIST1.1 criteria. Patient clinicopathological features are summarized in Fig. 1A and Supplementary Table 1. Examination of the patients' clinical parameters showed that responders and nonresponders presented highly significant differences in overall survival (Fig. 1B). Both the tumor differentiation status and tumor stage, location, and size showed no significant difference between the two cohorts; additionally, the sex and age of patients showed no association with response (Fig. 1C). For proteomic analysis, we dissected gastric cancer regions with > 80% tumor cells; 10,210 nonredundant proteins were quantified, and ~ 3,949 proteins (Supplementary Table 2) identified in at least 50% of the samples were subjected to downstream statistical analyses. There were no major differences in the coverage between the responders and nonresponders (Fig. 1D, E; Supplementary Tables 3 and 4).

Functional analysis of responders and nonresponders to trastuzumab therapy

We addressed whether proteomics features would differentiate between responders versus nonresponders with gastric carcinomas sampled prior to trastuzumab therapy. We first found 421 differentially expressed proteins (DEPs) after we applied low stringency Student's *t* tests with a p value cutoff (p value < 0.05) and fold change > 2 between responders and nonresponders (Fig. 2A, Supplementary Table 5), and the top 50 up- and downregulated DEPs in responders and nonresponders were shown as a histogram in Supplementary Fig. 1. Then, we constructed proteomaps to cluster the DEPs according to KEGG pathway annotations and found that the responder cluster was enriched in translation-related

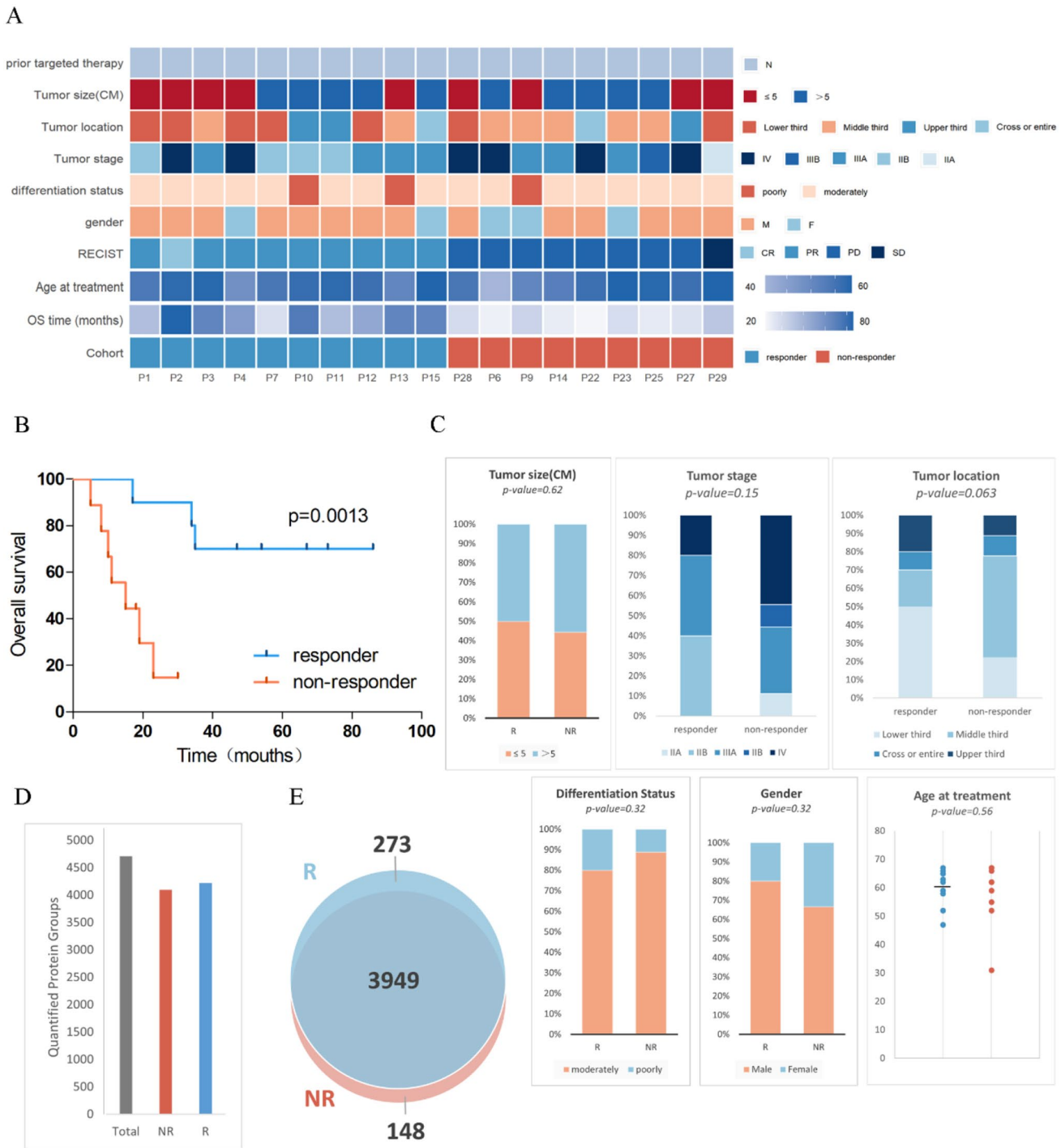

Fig. 1 Proteomics landscape of gastric carcinoma response to trastuzumab therapy. **A** The study cohort of responders and nonresponders undergoing trastuzumab therapy and clinical parameters are indicated in the heatmap. **B** Overall survival (OS) showed highly significant differences between responders and nonresponders to trastuzumab therapy according to Kaplan–Meier estimates. **C** The following clinical parameters were examined for the datasets: tumor size; differentiation status; tumor location; and tumor stage. **D** Total number of proteins quantified in each cohort of samples. **E** A Venn diagram showing the overlap of quantified proteins in each cohort. Abbreviations are as follows: *M* male, *F* female, *CR* complete response, *PR* partial response, *PD* progressive disease, *SD* stable disease, *R* responders, *NR* nonresponders

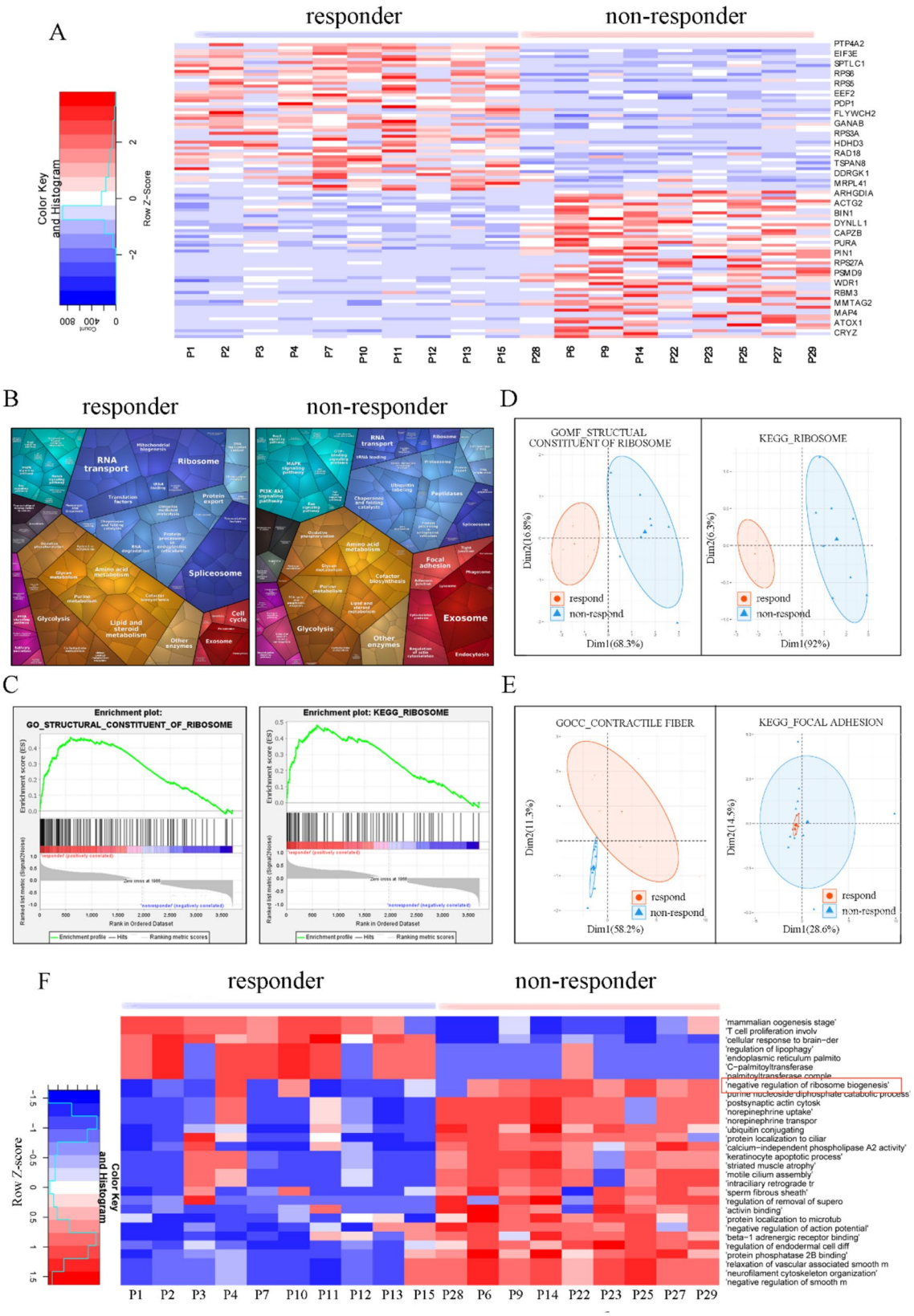
A
responder
non-responder
Color Key and Histogram
Row Z-Score
PTP4A2
EIF3E
SPTLC1
RPS6
RPS6
EEF2
PDP1
FLYWCH2
GANAB
RPS3A
HDHD3
RAD18
TSPAN8
DDRGK1
MRPL41
ARHGDIA
ACTG2
BIN1
DYNLL1
CAPZB
PURA
PIN1
RPS27A
PSMD9
WDR1
RBM3
MMTAG2
MAP4
ATOX1
CRYZ
P1 P2 P3 P4 P7 P10 P11 P12 P13 P15 P28 P6 P9 P14 P22 P23 P25 P27 P29
B
responder
non-responder
RNA transport
Ribosome
Spliceosome
Amino acid metabolism
Glycolysis
Lipid and steroid metabolism
Cell cycle
Exosome
Focal adhesion
Other enzymes
D
GOMF_STRUCTUAL CONSTITUENT OF RIBOSOME
KEGG_RIBOSOME
Dim2(16.8%)
Dim1(68.3%)
Dim2(6.3%)
Dim1(92%)
respond
non-respond
C
Enrichment plot: GO_STRUCTURAL_CONSTITUENT_OF_RIBOSOME
Enrichment plot: KEGG_RIBOSOME
Enrichment score (ES)
Ranked list metric (Signal2Noise)
Rank in Ordered Dataset
Enrichment profile
Hits
Ranking metric scores
E
GOCC_CONTRACTILE FIBER
KEGG_FOCAL ADHESION
Dim2(11.3%)
Dim1(58.2%)
Dim2(14.5%)
Dim1(28.6%)
respond
non-respond
F
responder
non-responder
Row Z-score
Color Key and Histogram
'mammalian oogenesis stage'
'T cell proliferation involv
'cellular response to brain−der
'regulation of lipophagy'
'endoplasmic reticulum palmito
'C−palmitoyltransferase
'palmitoyltransferase comple
'negative regulation of ribosome biogenesis'
'purine nucleoside diphosphate catabolic process'
'postsynaptic actin cytosk
'norepinephrine uptake'
'norepinephrine transpor
'ubiquitin conjugating
'protein localization to ciliar
'calcium−independent phospholipase A2 activity'
'keratinocyte apoptotic process'
'striated muscle atrophy'
'motile cilium assembly'
'intraciliary retrograde tr
'sperm fibrous sheath'
'regulation of removal of supero
'activin binding'
'protein localization to microtub
'negative regulation of action potential'
'beta−1 adrenergic receptor binding'
'regulation of endodermal cell diff
'protein phosphatase 2B binding'
'relaxation of vascular associated smooth m
'neurofilament cytoskeleton organization'
'negative regulation of smooth m
P1 P2 P3 P4 P7 P10 P11 P12 P13 P15 P28 P6 P9 P14 P22 P23 P25 P27 P29

◂**Fig. 2** Functional differences between responders and nonresponders to trastuzumab therapy. **A** Heatmap of anti-HER2 signature proteins showing discrimination between responders and nonresponders. **B** Functional categories in responders and nonresponders, as illustrated using Proteomaps. **C** GSEA of the differentially expressed proteins in responders. **D** Principal component analysis (PCA) shows excellent separation between responders and nonresponders based on the responder signature proteins. **E** PCA shows little separation, even overlap, between responders and nonresponders based on the nonresponder signature proteins. **F** GSVA revealed that ribosome biogenesis was correlated with a lack of response to treatment

proteins, whereas the nonresponder cluster was enriched in signal transduction proteins (Supplementary Fig. 2A).

Among the translation categories, responders had higher proportions of ribosome proteins and RNA transport proteins. However, in the signal transduction categories, nonresponders had higher proportions of proteins related to the PI3K/AKT and MAPK signaling pathways (Fig. 2B), which play important roles in the response to HER2-targeted therapy [17–20].

To assess biologic pathway-level patterns in the responder and nonresponder datasets, we applied GSEA to the entire expression data to discover significantly enriched protein groups. GSEA showed that the responders were mainly associated with the molecular function of structural constituent of ribosome, the biological process of viral gene expression, the cellular components of ribosome and proteasome, and the KEGG pathway of protein export (Fig. 2C and Supplementary Fig. 2B). The nonresponders presented the protein signatures of contractile fibers and the focal adhesion signaling pathway (Supplementary Fig. 2C). To establish the core biological pathway underlying the response to treatment, enriched GO term and KEGG pathway data were explored by principal component analyses (PCAs). The PCAs showed that the two groups clustered separately, revealing that the structural constituents of the ribosome and ribosome KEGG pathways discriminated responders and nonresponders into two significantly distinct groups (Fig. 2D, E and Supplementary Fig. 2D). Notably, GSVA revealed that negative regulation of ribosome biogenesis stood out in nonresponders (Fig. 2F). The results of these data indicated that ribosomal proteins (RPs) have a high correlation with the sensitivity to trastuzumab in gastric carcinoma.

Identification of key proteins associated with the response to trastuzumab therapy

Deeper analysis of the most differentially expressed proteins involved in structural constituent of the ribosome and ribosome GO terms and KEGG pathways was performed, and hierarchical clustering showed that multiple ribosomal protein small (RPS) and ribosomal protein large (RPL) subunit proteins appear to be regulated in responders and nonresponders (Fig. 3A). We found an intriguing consistency in the hierarchical clustering based on GO and KEGG results, and RPS6 was the most differentially expressed protein between responders and nonresponders (Supplementary Table 6A and 6B); RPS6 is a component of the 40S small ribosomal subunit and participates in the control of mRNA translation [21], and its activation is related to the development of trastuzumab-resistant clones of gastric carcinoma cell lines [22]. In our data, we found that RPS6 expression was slightly higher in responders than in nonresponders (p value = 0.0485) (Supplementary Fig. 3A, B), whereas obviously strong phosphorylation of RPS6 (p-RPS6) was observed in nonresponders than in responders (p value = 0.0072) (Fig. 3B, C). Further analysis showed that the ribosomal protein S6 kinase RPS6KA1, which can phosphorylate RPS6, was especially higher in nonresponders (Supplementary Fig. 3C), and the result was consistent with the Oncomine dataset GSE141352 (Supplementary Fig. 3D).

To further explore the prognostic value of RPS6 and p-RPS6 related to trastuzumab antitumor efficacy, we conducted a survival analysis of these two proteins in our subgroup and the TCGA dataset. We found that a high level of RPS6 was insignificantly associated with the prognosis of GC patients who were treated with trastuzumab therapy (p value = 0.3593) (Fig. 3D) and in patients in the TCGA stomach adenocarcinoma cohort (p value = 0.47) (Supplementary Fig. 3E). Moreover, RPS6 was not differentially expressed between normal and gastric carcinoma tissues in TCGA samples (p value = 0.9939) (Supplementary Fig. 3F). However, a high level of p-RPS6 was significantly associated with a lower overall survival rate in our subgroup analysis (p value = 0.0098) (Fig. 3E). These results suggested that phosphorylated ribosomal S6 is probably a key protein associated with the response to trastuzumab therapy.

Phosphorylated ribosomal S6 inhibits trastuzumab antitumor efficacy by triggering the AKT/mTOR/RPS6 signaling pathway

Since RPS6 is also a downstream effector of PI3K/AKT/mTOR signaling, we aimed to induce decreased phosphorylated RPS6 in cell culture; we treated gastric carcinoma cell lines with GSK458 (omipalisib), a potent inhibitor of mTOR, which was first applied in a human phase I study in patients with advanced solid tumor malignancies [23]. To test the inhibitory effect of GSK458 on the activation

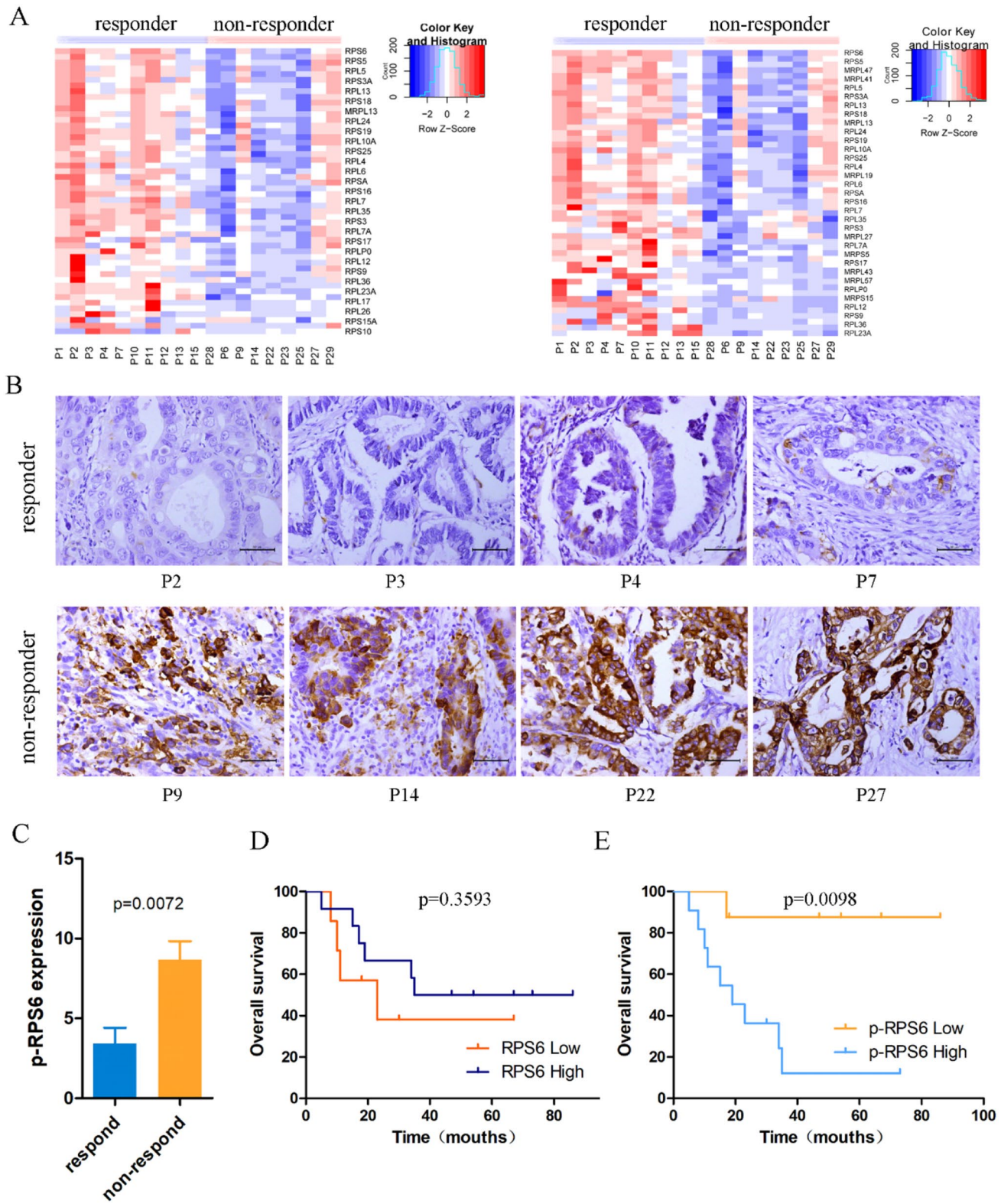

Fig. 3 Activation of RPS6 is associated with the response to trastuzumab therapy. **A** Heatmap depicting the expression profiling of the responder DEPs based on GO and KEGG enrichment analyses. **B** Examples of IHC staining of p-RPS6 expression in responders and nonresponders. Scale bar: 50 μm. **C** Boxplot showing the quantification of the IHC staining results. **D** Overall survival of anti-HER2-treated patients with low or high expression of RPS6. **E** Overall survival of anti-HER2-treated patients with low or high expression of p-RPS6. *p* value, log-rank test

of RPS6 in HER2-positive GC cells, we treated NCI-N87 and SNU216 cells with increasing concentrations of GSK458 for 24 h. The western blotting data in Fig. 4A implied that the persistence of HER2 expression in NCI-N87 and SNU216 cells, and the level of phosphorylated RPS6 was significantly decreased with 100 nM GSK458 in all cells. Then, we attempted to determine whether inhibition of phosphorylated RPS6 could improve trastuzumab antitumor efficacy. We treated two types of GC cells with either single GSK458 or trastuzumab or their combination for ~ 120 h and then measured cell viability by CCK-8 assay. As shown in Fig. 4B, the combination of GSK458 and trastuzumab markedly reduced the viability of SNU216 cells, and this effect was statistically significant at 120 h with trastuzumab alone and with the combination of GSK458 and trastuzumab. A similar trend was observed in NCI-N87 cells. To assess whether RPS6 activation is a mechanism that may induce mTOR inhibition, western blotting was conducted to analyze AKT and p-AKT levels in SNU216 and NCI-N87 cells following exposure to GSK458 or trastuzumab or their combination for 24 h and 96 h (Fig. 4C). As anticipated, p-RPS6 (Ser240/244) levels in GC cells decreased when p-AKT (Ser473) levels were further decreased after GSK458 treatment. The levels of p-AKT (Ser473) and p-RPS6 (Ser240/244) proteins were also marginally decreased by the trastuzumab/GSK458 combination. Trastuzumab alone could not suppress the expression of p-AKT in either SNU216 or NCI-N87 cells.

To further validate the activation of RPS6 was a key inhibitory site in trastuzumab antitumor efficacy, we performed loss- and gain-of-function methods to deplete or overexpress RPS6, leading to decreased or upregulated expression of phosphorylated RPS6 in GC cells, respectively (Fig. 4D). CCK-8 assay revealed that RPS6-knockdown dramatically inhibited GC cells proliferation when treated with trastuzumab alone compared with ctrl cells (Fig. 4E). The cell proliferation was not inhibited by treating with trastuzumab alone when RPS6 was overexpressed in the cells, but significantly inhibited by treatment with combination of trastuzumab and GSK458 which is supposed to inhibit the activated RPS6 protein (p-RPS6) directly [22] (Fig. 4F). These data suggest that p-RPS6 was a key effector of resistance to trastuzumab efficacy.

Next, we developed a mouse model to examine whether p-RPS6 could be responsible for trastuzumab efficacy in vivo. NCI-N87 cells were subcutaneously implanted in BALB/c nude mice that were randomized and treated with either trastuzumab, GSK458, a combination of both, or the control agents. Compared with control group, trastuzumab or GSK458 treatment alone was found to be mildly effective in tumor progression, whereas trastuzumab/GSK458 combination significantly reduced the tumor growth in vivo (Fig. 5A–C). Using immunohistochemistry (IHC) staining of sacrifice tumors, we confirmed that p-RPS6 was significantly decreased in protein abundance in trastuzumab/GSK458 combination therapy group (Fig. 5D–F). Consistently, the AKT/mTOR/RPS6 signaling pathway was also inhibited. We found that p-AKT and p-RPS6 was significantly decreased in combination group, but no notably change was observed for the levels of AKT and RPS6 in all groups (Fig. 5G). These data suggested the potential of p-RPS6 to inhibit the efficacy of trastuzumab by triggering the mTOR signaling pathway.

According to our data, p-RPS6 was highly expressed in nonresponder tumor samples, suggesting its important role in resistance. When the phosphorylation of RPS6 and AKT was inhibited and cancer cell viability was significantly decreased, which was responsible for trastuzumab sensitivity in vivo and in vitro assays, and also confirmed the activation of the AKT/mTOR/RPS6 pathway in blocking trastuzumab antitumor efficacy (Fig. 6).

Discussion

Currently, only three molecular biomarkers have been demonstrated to predict a response to targeted therapies in patients with GC: HER2, microsatellite instability (MSI) status, and PD-L1 expression [24]. Nevertheless, based on the biomarker of HER2 expression, only trastuzumab and trastuzumab deruxtecan (T-DXd) are being used in routine clinical practice for advanced gastric carcinoma patients [5, 25]. T-DXd is a novel HER2-targeted antibody–drug conjugate approved for advanced or metastatic GC patients who have received a prior trastuzumab-based regimen by the United States Food and Drug Administration in 2021 [25, 26]. However, based on several factors (the pronounced benefit in the HER2 IHC 3 + population, the lower response rate in HER2 IHC 2 + or ISH-positive GC patients, and the limited ethnic diversity and adverse events related to underlying lung injury in the DESTINY-Gastric01 study [25, 27–29]), trastuzumab plus chemotherapy remains the standard first-line targeted therapy with HER2-positive advanced GC patients since the publication of the landmark ToGA trial [5, 30].

Unfortunately, not all HER2-positive GC patients benefit from treatment with trastuzumab therapy because of initial or acquired resistance [31, 32]. Although transcriptomic and targeted sequencing analyses in cell lines, plasma and tissue biopsy samples have been used for further examination of potential biomarkers to predict trastuzumab benefit [17, 33–35], the proteomic landscape of tissue samples

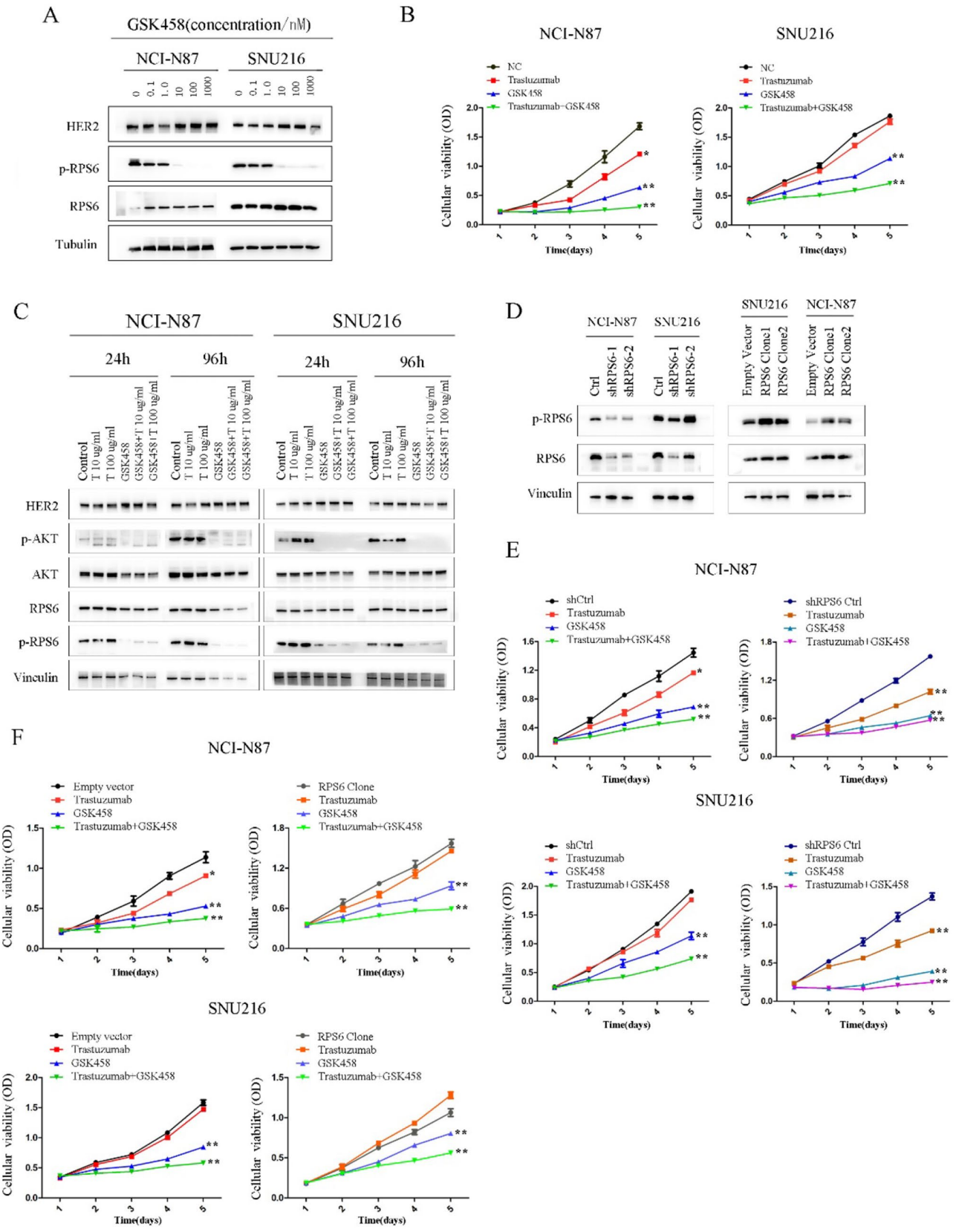
A
GSK458(concentration/nM)
NCI-N87
SNU216
0 0.1 1.0 10 100 1000
HER2
p-RPS6
RPS6
Tubulin
B
NCI-N87
SNU216
NC
Trastuzumab
GSK458
Trastuzumab+GSK458
Cellular viability (OD)
Time(days)
C
NCI-N87
SNU216
24h
96h
Control
T 10 ug/ml
T 100 ug/ml
GSK458
GSK458+T 10 ug/ml
GSK458+T 100 ug/ml
HER2
p-AKT
AKT
RPS6
p-RPS6
Vinculin
D
NCI-N87
SNU216
Ctrl
shRPS6-1
shRPS6-2
Empty Vector
RPS6 Clone1
RPS6 Clone2
p-RPS6
RPS6
Vinculin
E
NCI-N87
SNU216
shCtrl
shRPS6 Ctrl
Trastuzumab
GSK458
Trastuzumab+GSK458
Cellular viability (OD)
Time(days)
F
NCI-N87
SNU216
Empty vector
RPS6 Clone
Trastuzumab
GSK458
Trastuzumab+GSK458
Cellular viability (OD)
Time(days)

◂**Fig. 4** Validation of p-RPS6 triggering AKT/mTOR/RPS6 signaling and inhibiting trastuzumab antitumor efficacy in vitro. **A** The levels of p-rpS6 in GC cell lines treated with GSK458 (0.1, 1, 10, 100, 1000 μmol). **B** Effect of trastuzumab and/or GSK458 on the viability of GC cell lines. Cell viability was determined via a CCK-8 cell proliferation assay and expressed as the mean ± SD ($n = 3$), *$p < 0.01$, **$p < 0.001$. **C** AKT/mTOR biomarker modulation by trastuzumab and/or GSK458 in GC cell lines for 24 h and 96 h. **D** RPS6 and p-RPS6 protein expression in GC cells transfected with corresponding shRNAs (left) or overexpression vector (right). **E**, **F** Effect of trastuzumab and/or GSK458 on the viability of RPS6-knockdown (**E**) and RPS6-overpressed (**F**) GC cells. Cell viability was determined via a CCK-8 cell proliferation assay and expressed as the mean ± SD ($n = 3$), *$p < 0.01$, **$p < 0.001$

of patients treated with trastuzumab is still sparse. Herein, we presented the MS-based proteomic profiles of 38 samples from 19 advanced GC patients pretreated with trastuzumab and generated a dataset of differentially expressed proteins and functional alterations between responders and nonresponders.

We found that the DEPs of responders were enriched in the ribosome KEGG pathway, which was highly consistent with the GO analysis results. As an indispensable ribosomal protein, RPS6 was the most upregulated protein in our proteomic dataset. However, this increase was not significant between responders and nonresponders in the immunohistochemistry confirmation study. Numerous studies have demonstrated that RPS6, which was the first identified posttranslational modification of the ribosome, is subject to phosphorylation in response to multiple pathological stimuli [36], and S6K is the predominant rpS6 kinase [37]. Notably, we found that ribosomal protein S6 kinase A1 (RPS6KA1) was highly expressed in nonresponders. This is consistent with findings from the molecular effects of trastuzumab on kinase activity by RNA-sequencing analysis available in the GEO repository (accession GSE141352). The gene expression of RPS6KA1 was significantly upregulated in nonresponder GC cells [38]. We then compared the expression of p-RPS6 across responders and nonresponders and found dramatically increased expression of p-RPS6 in nonresponders. In vitro, we also evaluated the effect of p-RPS6 on cell viability in HER2-positive GC cell lines. The mTOR inhibitor GSK458 efficiently inhibited phosphorylation of the downstream effector RPS6, and GSK458 in combination with trastuzumab could more effectively inhibit cancer cell growth than trastuzumab treatment alone. Previous studies based on trastuzumab-resistant clones derived from HER2-amplified GC cell lines showed that RPS6 activation was related to anti-HER2 drug resistance [39, 40]. In addition, our data showed that overexpression of RPS6 was not significantly associated with poorer overall survival in GC patients, which is consistent with the results of TCGA database analysis (high, $n = 92$; low/medium, $n = 300$) [41]. Conversely, we found that patients with overexpression of p-RPS6 had obviously shorter overall survival than patients with low expression. Thus, our data indicate that low levels of phosphorylated RPS6 are significantly associated with a durable response and better survival after anti-HER2 therapy.

We mainly found that phosphorylated RPS6 levels were obviously different between responders and nonresponders, and that the PI3K/mTOR pathway was altered significantly. p-RPS6 is a common downstream effector of the ribosome and PI3K/mTOR pathways [39, 42]. The phosphorylated (activated) form of RPS6 is a commonly used readout for mTORC1 activity [21, 43]. In recent years, there has been more focus on the association between the PI3K/Akt/mTOR signaling pathway and trastuzumab resistance in breast cancer than in gastric cancer [44–47]. Genomic analysis showed that PI3K/Akt/mTOR signaling activation in GC patients treated with trastuzumab was associated with poor outcomes in terms of both OS and PFS [48]. In trastuzumab-stable resistant clones of HER2-amplified GC cell lines, the PI3K/AKT/mTOR/RPS6 signaling pathway was persistently activated to sustain tumor growth and a more aggressive phenotype [39]. Thus, our investigation indicated that AKT/mTOR/RPS6 signaling activation of GC patients pretreated might less benefit from trastuzumab and be at a higher risk of resistance.

Inhibitors targeting only mTOR have limited treatment efficacy owing to incomplete inhibition or compensatory activation of AKT [49, 50]. Here, we observed that the PI3K/mTOR dual inhibitor GSK458 efficiently inhibited downstream effectors, induced AKT and RPS6 dephosphorylation, and inhibited GC cell growth and proliferation, especially in combination with trastuzumab. Consequently, the combination of trastuzumab and mTOR inhibitors provided evidence of effective treatment for pretreatment GC tumors with AKT/mTOR/RPS6 signaling activation.

This study highlights the application of quantitative proteomics data generated from tissue samples of pretreatment GC patients to identify the potential determinants of response to trastuzumab. Our proteomic analyses and studies demonstrate that phosphorylated RPS6 could trigger AKT/mTOR/RPS6 signaling, which inhibits the sensitivity of GC patients to trastuzumab and is associated with poor survival after anti-HER2 therapy. Targeting RPS6 dephosphorylation could significantly suppress GC cell survival, which highlights the broad potential of targeting the AKT/mTOR/RPS6 axis with effective inhibitors in combination with trastuzumab. Overall, our findings reveal that GC patients with low expression of p-RPS6 in tumor tissue are more likely to benefit from trastuzumab therapy than those with high expression. Moreover, patients with high expression of p-RPS6 may benefit from trastuzumab

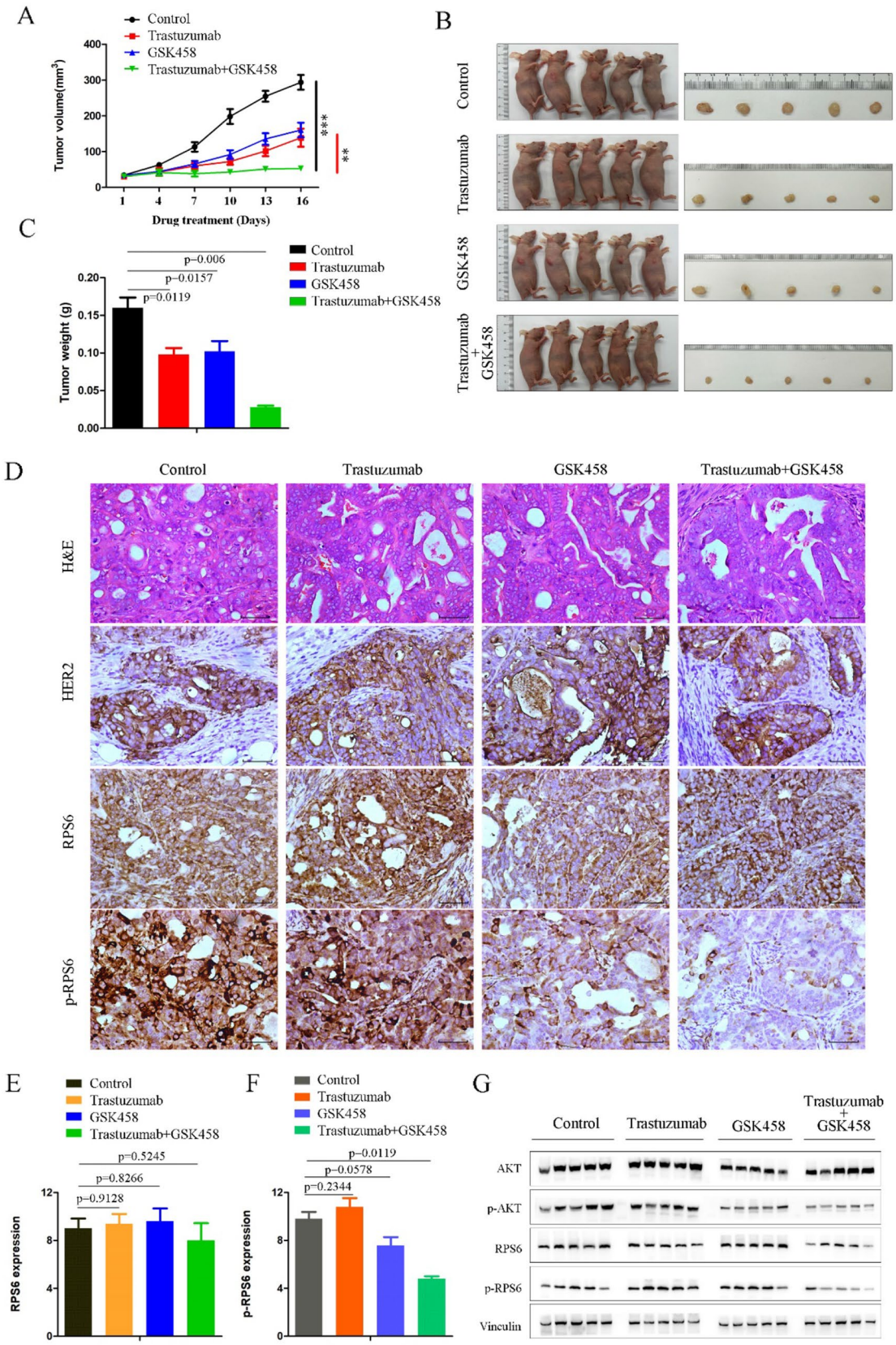
A
Control
Trastuzumab
GSK458
Trastuzumab+GSK458
Tumor volume(mm³)
Drug treatment (Days)
***
**
B
Control
Trastuzumab
GSK458
Trastuzumab + GSK458
C
Control
Trastuzumab
GSK458
Trastuzumab+GSK458
p=0.006
p=0.0157
p=0.0119
Tumor weight (g)
D
Control
Trastuzumab
GSK458
Trastuzumab+GSK458
H&E
HER2
RPS6
p-RPS6
E
Control
Trastuzumab
GSK458
Trastuzumab+GSK458
p=0.5245
p=0.8266
p=0.9128
RPS6 expression
F
Control
Trastuzumab
GSK458
Trastuzumab+GSK458
p=0.0119
p=0.0578
p=0.2344
p-RPS6 expression
G
Control
Trastuzumab
GSK458
Trastuzumab + GSK458
AKT
p-AKT
RPS6
p-RPS6
Vinculin

◂**Fig. 5** P-RPS6 inhibits the efficacy of trastuzumab by activating AKT/mTOR/RPS6 signaling in vivo. **A** The tumor volume growth curves of mice after injected NCI-N87 cells treated with trastuzumab, GSK458, or trastuzumab/ GSK458 for 16 days. $*p<0.001$, $**p<0.0001$. **B** Images of tumors formed after different treatment. **C** Tumor weight of mice after different treatment. **D** Representative H&E staining images of the tumors and HER2, RPS6, and p-RPS6 protein expression detected by IHC analysis. Images were captured under 40X (inset) magnification. Scale bars = 50 μm. **E**, **F** Boxplot showing the quantification of the IHC staining results of RPS6 and p-RPS6, respectively. **G** Immunoblot analysis of AKT, p-AKT, RPS6, and p-RPS6 in whole protein extracts of tumors

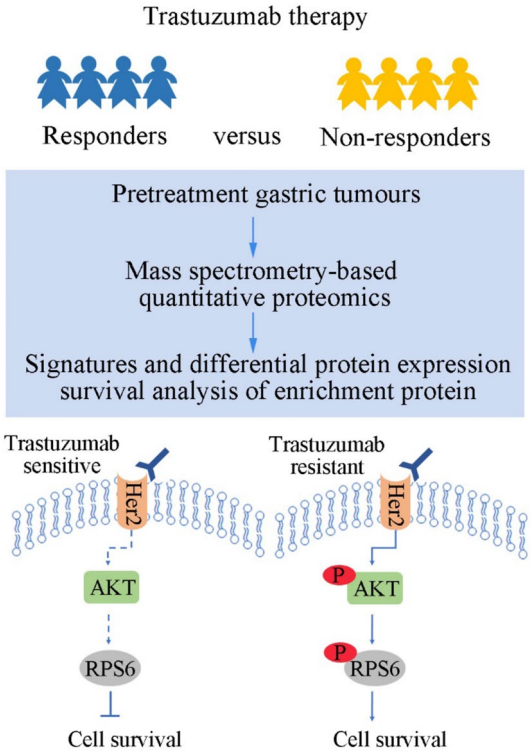

Fig. 6 A scheme of the proposed mechanism by which phosphorylated RPS6 blocks trastuzumab antitumor efficacy

in combination with RPS6 phosphorylation inhibitors to obtain a durable response and better survival.

Supplementary Information The online version contains supplementary material available at https://doi.org/10.1007/s00280-023-04571-2.

Acknowledgements This work was supported by the Shanghai Municipal Key Clinical Specialty (shslczdzk01303), National Natural Science Foundation of China (NO81372637, NO12171275, and NO81972326), First Round of 3-year Action Plan to Promote Clinical Skills and Clinical Innovation in Municipal Hospitals of Shanghai (16CR2039B). Tsinghua University Spring Breeze Fund (2020Z99CFY044), and Tsinghua University Education Foundation Fund (042202008).

Data availability The data will be made available on reasonable request.

Declarations

Conflict of interest The authors declare that they have no competing interests.

Ethical approval This study was approved by the Ethics Committee of Shanghai General Hospital, Shanghai Jiao Tong University School of Medicine (Ethics No. 2016KY161-3).

References

1. Chen WQ, Zheng RS, Baade PD, Zhang SW, Zeng HM, Bray F et al (2016) Cancer statistics in China, 2015. Ca-Cancer J Clin 66:115–132
2. Van Cutsem E, Bang YJ, Feng-Yi F, Xu JM, Lee KW, Jiao SC et al (2015) HER2 screening data from ToGA: targeting HER2 in gastric and gastroesophageal junction cancer. Gastric Cancer 18:476–484
3. Matsusaka S, Nashimoto A, Nishikawa K, Miki A, Miwa H, Yamaguchi K et al (2016) Clinicopathological factors associated with HER2 status in gastric cancer: results from a prospective multicenter observational cohort study in a Japanese population (JFMC44-1101). Gastric Cancer 19:839–851
4. Sheng WQ, Huang D, Ying JM, Lu N, Wu HM, Liu YH et al (2013) HER2 status in gastric cancers: a retrospective analysis from four Chinese representative clinical centers and assessment of its prognostic significance. Ann Oncol 24:2360–2364
5. Bang YJ, Van Cutsem E, Feyereislova A, Chung HC, Shen L, Sawaki A et al (2010) Trastuzumab in combination with chemotherapy versus chemotherapy alone for treatment of HER2-positive advanced gastric or gastro-oesophageal junction cancer (ToGA): a phase 3, open-label, randomised controlled trial. Lancet 376:687–697
6. Group G, Paoletti X, Oba K, Burzykowski T, Michiels S, Ohashi Y et al (2010) Benefit of adjuvant chemotherapy for resectable gastric cancer: a meta-analysis. JAMA 303:1729–1737
7. Makiyama A, Sukawa Y, Kashiwada T, Kawada J, Hosokawa A, Horie Y et al (2020) Randomized, phase II study of trastuzumab beyond progression in patients with HER2-positive advanced gastric or gastroesophageal junction cancer: WJOG7112G (T-ACT Study). J Clin Oncol 38:1919–1927
8. Smyth EC, Nilsson M, Grabsch HI, van Grieken NC, Lordick F (2020) Gastric cancer. Lancet 396:635–648
9. Cancer Genome Atlas Research N (2014) Comprehensive molecular characterization of gastric adenocarcinoma. Nature 513:202–209
10. Joshi SS, Badgwell BD (2021) Current treatment and recent progress in gastric cancer. CA Cancer J Clin 71:264–279
11. Suhre K, McCarthy MI, Schwenk JM (2021) Genetics meets proteomics: perspectives for large population-based studies. Nat Rev Genet 22:19–37
12. Manzoni C, Kia DA, Vandrovcova J, Hardy J, Wood NW, Lewis PA et al (2018) Genome, transcriptome and proteome: the rise of omics data and their integration in biomedical sciences. Brief Bioinform 19:286–302
13. Liu W, Chang J, Liu M, Yuan J, Zhang J, Qin J et al (2017) Quantitative proteomics profiling reveals activation of mTOR pathway in trastuzumab resistance. Oncotarget 8:45793–45806
14. Duarte HO, Rodrigues JG, Gomes C, Hensbergen PJ, Ederveen ALH, de Ru AH et al (2021) ST6Gal1 targets the ectodomain of ErbB2 in a site-specific manner and regulates gastric cancer cell sensitivity to trastuzumab. Oncogene 40:3719–3733

15. Keller S, Zwingenberger G, Ebert K, Hasenauer J, Wasmuth J, Maier D et al (2018) Effects of trastuzumab and afatinib on kinase activity in gastric cancer cell lines. Mol Oncol 12:441–462
16. An E, Ock CY, Kim TY, Lee KH, Han SW, Im SA et al (2017) Quantitative proteomic analysis of HER2 expression in the selection of gastric cancer patients for trastuzumab treatment. Ann Oncol 28:110–115
17. Mezynski MJ, Farrelly AM, Cremona M, Carr A, Morgan C, Workman J et al (2021) Targeting the PI3K and MAPK pathways to improve response to HER2-targeted therapies in HER2-positive gastric cancer. J Transl Med 19:184
18. Adam-Artigues A, Arenas EJ, Martinez-Sabadell A, Braso-Maristany F, Cervera R, Tormo E et al (2022) Targeting HER2-AXL heterodimerization to overcome resistance to HER2 blockade in breast cancer. Sci Adv 8:eabk2746
19. Dave B, Migliaccio I, Gutierrez MC, Wu MF, Chamness GC, Wong H et al (2011) Loss of phosphatase and tensin homolog or phosphoinositol-3 kinase activation and response to trastuzumab or lapatinib in human epidermal growth factor receptor 2-overexpressing locally advanced breast cancers. J Clin Oncol 29:166–173
20. Butti R, Das S, Gunasekaran VP, Yadav AS, Kumar D, Kundu GC (2018) Receptor tyrosine kinases (RTKs) in breast cancer: signaling, therapeutic implications and challenges. Mol Cancer 17:34
21. Yi YW, You KS, Park JS, Lee SG, Seong YS (2021) Ribosomal protein S6: a potential therapeutic target against cancer? Int J Mol Sci 23:48
22. Gambardella V, Gimeno-Valiente F, Tarazona N, Martinez-Ciarpaglini C, Roda D, Fleitas T et al (2019) NRF2 through RPS6 activation is related to anti-HER2 drug resistance in HER2-amplified gastric cancer. Clin Cancer Res 25:1639–1649
23. Munster P, Aggarwal R, Hong D, Schellens JH, van der Noll R, Specht J et al (2016) First-in-human phase I study of GSK2126458, an oral pan-class I phosphatidylinositol-3-kinase inhibitor, in patients with advanced solid tumor malignancies. Clin Cancer Res 22:1932–1939
24. Nakamura Y, Kawazoe A, Lordick F, Janjigian YY, Shitara K (2021) Biomarker-targeted therapies for advanced-stage gastric and gastro-oesophageal junction cancers: an emerging paradigm. Nat Rev Clin Oncol 18:473–487
25. Shitara K, Bang YJ, Iwasa S, Sugimoto N, Ryu MH, Sakai D et al (2020) Trastuzumab deruxtecan in previously treated HER2-positive gastric cancer. New Engl J Med 382:2419–2430
26. Shitara K, Iwata H, Takahashi S, Tamura K, Park H, Modi S et al (2019) Trastuzumab deruxtecan (DS-8201a) in patients with advanced HER2-positive gastric cancer: a dose-expansion, phase 1 study. Lancet Oncol 20:827–836
27. Yamaguchi K, Bang YJ, Iwasa S, Sugimoto N, Ryu MH, Sakai D et al (2020) Trastuzumab deruxtecan (T-DXd; DS-8201) in patients with HER2-low, advanced gastric or gastroesophageal junction (GEJ) adenocarcinoma: Results of the exploratory cohorts in the phase II, multicenter, open-label DESTINY-Gastric01 study. Ann Oncol 31:S899–S900
28. Aoki M, Iwasa S, Boku N (2021) Trastuzumab deruxtecan for the treatment of HER2-positive advanced gastric cancer: a clinical perspective. Gastric Cancer 24:567–576
29. Tsurutani J, Iwata H, Krop I, Janne PA, Doi T, Takahashi S et al (2020) Targeting HER2 with trastuzumab deruxtecan: a dose-expansion, phase I study in multiple advanced solid tumors. Cancer Discov 10:688–701
30. Siena S, Marsoni S, Sartore-Bianchi A (2020) Breaking barriers in HER2+ cancers. Cancer Cell 38:317–319
31. Rivera F, Romero C, Jimenez-Fonseca P, Izquierdo-Manuel M, Salud A, Martinez E et al (2019) Phase II study to evaluate the efficacy of Trastuzumab in combination with Capecitabine and Oxaliplatin in first-line treatment of HER2-positive advanced gastric cancer: HERXO trial. Cancer Chemother Pharmacol 83:1175–1181
32. Zhu Y, Zhu X, Wei X, Tang C, Zhang W (2021) HER2-targeted therapies in gastric cancer. Biochim Biophys Acta Rev Cancer 1876:188549
33. Wang DS, Liu ZX, Lu YX, Bao H, Wu X, Zeng ZL et al (2019) Liquid biopsies to track trastuzumab resistance in metastatic HER2-positive gastric cancer. Gut 68:1152–1161
34. Janjigian YY, Sanchez-Vega F, Jonsson P, Chatila WK, Hechtman JF, Ku GY et al (2018) Genetic predictors of response to systemic therapy in esophagogastric cancer. Cancer Discov 8:49–58
35. Ebert K, Haffner I, Zwingenberger G, Keller S, Raimundez E, Geffers R et al (2022) Combining gene expression analysis of gastric cancer cell lines and tumor specimens to identify biomarkers for anti-HER therapies-the role of HAS2. SHB and HBEGF BMC Cancer 22:254
36. Meyuhas O (2015) Ribosomal protein S6 phosphorylation: four decades of research. Int Rev Cell Mol Biol 320:41–73
37. Bohlen J, Roiuk M, Teleman AA (2021) Phosphorylation of ribosomal protein S6 differentially affects mRNA translation based on ORF length. Nucleic Acids Res 49:13062–13074
38. Ebert K, Zwingenberger G, Barbaria E, Keller S, Heck C, Arnold R et al (2020) Determining the effects of trastuzumab, cetuximab and afatinib by phosphoprotein, gene expression and phenotypic analysis in gastric cancer cell lines. BMC Cancer 20:1039
39. Gambardella V, Gimeno-Valiente F, Tarazona N, Ciarpaglini CM, Roda D, Fleitas T et al (2019) NRF2 through RPS6 activation is related to anti-HER2 drug resistance in HER2-amplified gastric cancer. Clin Cancer Res 25:1639–1649
40. Yang-Kolodji G, Mumenthaler SM, Mehta A, Ji LY, Tripathy D (2015) Phosphorylated ribosomal S6 (p-rpS6) as a post-treatment indicator of HER2 signalling targeted drug resistance. Biomarkers 20:313–322
41. Chandrashekar DS, Karthikeyan SK, Korla PK, Patel H, Shovon AR, Athar M et al (2022) UALCAN: an update to the integrated cancer data analysis platform. Neoplasia 25:18–27
42. Pelletier J, Thomas G, Volarevic S (2018) Ribosome biogenesis in cancer: new players and therapeutic avenues. Nat Rev Cancer 18:51–63
43. Magnuson B, Ekim B, Fingar DC (2012) Regulation and function of ribosomal protein S6 kinase (S6K) within mTOR signalling networks. Biochem J 441:1–21
44. Satpathy S, Jaehnig EJ, Krug K, Kim BJ, Saltzman AB, Chan DW et al (2020) Microscaled proteogenomic methods for precision oncology. Nat Commun 11:532
45. Morrow PK, Wulf GM, Ensor J, Booser DJ, Moore JA, Flores PR et al (2011) Phase I/II study of trastuzumab in combination with everolimus (RAD001) in patients with HER2-overexpressing metastatic breast cancer who progressed on trastuzumab-based therapy. J Clin Oncol 29:3126–3132
46. Hurvitz SA, Andre F, Jiang ZF, Shao ZM, Mano MS, Neciosup SP et al (2015) Combination of everolimus with trastuzumab plus paclitaxel as first-line treatment for patients with HER2-positive advanced breast cancer (BOLERO-1): a phase 3, randomised, double-blind, multicentre trial. Lancet Oncol 16:816–829
47. Andre F, O'Regan R, Ozguroglu M, Toi M, Xu BH, Jerusalem G et al (2014) Everolimus for women with trastuzumab-resistant, HER2-positive, advanced breast cancer (BOLERO-3): a randomised, double-blind, placebo-controlled phase 3 trial. Lancet Oncol 15:580–591
48. Diaz-Serrano A, Angulo B, Dominguez C, Pazo-Cid R, Salud A, Jimenez-Fonseca P et al (2018) Genomic profiling of HER2-positive gastric cancer: PI3K/Akt/mTOR pathway as predictor of

outcomes in HER2-positive advanced gastric cancer treated with trastuzumab. Oncologist 23:1092–1102
49. O'Reilly KE, Rojo F, She QB, Solit D, Mills GB, Smith D et al (2006) mTOR inhibition induces upstream receptor tyrosine kinase signaling and activates Akt. Cancer Res 66:1500–1508
50. Rozengurt E, Soares HP, Sinnet-Smith J (2014) Suppression of feedback loops mediated by PI3K/mTOR induces multiple overactivation of compensatory pathways: an unintended consequence leading to drug resistance. Mol Cancer Ther 13:2477–2488